

## Retrieving effective parameters for metamaterials at oblique incidence

Christoph Menzel,\* Carsten Rockstuhl, Thomas Paul, and Falk Lederer

*Institute of Condensed Matter Theory and Solid State Optics, Friedrich-Schiller-Universität Jena, D-07743 Jena, Germany*

Thomas Pertsch

*Institute of Applied Physics, Friedrich-Schiller-Universität Jena, D-07743 Jena, Germany*

(Received 17 January 2008; revised manuscript received 11 April 2008; published 29 May 2008)

We introduce a technique to retrieve effective metamaterial parameters for arbitrary angles of incidence. It employs the complex reflection and/or transmission coefficients of a finite slab. Explicit expressions for both polarizations are derived and the constraints to be met for obtaining unique solutions are discussed. The method is applied to the fishnet structure. It turns out that all retrieved parameters strongly depend on the lateral wave vector component due to the complexity of the metamaterial structure. Thus, these parameters are mere wave parameters rather than global material parameters. The physical effects behind this behavior are very likely anisotropy and spatial dispersion.

DOI: [10.1103/PhysRevB.77.195328](https://doi.org/10.1103/PhysRevB.77.195328)

PACS number(s): 78.20.Ci, 75.30.Kz, 73.20.Mf, 41.20.Jb

### I. INTRODUCTION

At the latest, Pendry's proposal<sup>1</sup> for a perfect lens in 2000 metamaterials (MMs) is attracting an ever increasing research interest (see, e.g., Ref. 2 and references therein). The proposed imaging system is based on a slab made of a material with both an isotropic permittivity and permeability equal to  $-1$  in the same spectral domain. For appropriate system parameters, information carried by all homogeneous and evanescent waves emanating from an object is perfectly restored in the image plane. The image is therefore identical to the object. The existence of such a lens would be of crucial importance to many fields, ranging from microscopic imaging of biological objects to photolithographic optics in the semiconductor industry. Whereas media with a negative permittivity are readily at hand, the latter property is not found in natural materials. Thus, the realization of media with negative permeability can be regarded as the *conditio sine qua non* for the practical implementation of a perfect lens. It is supposed that MMs can meet this requirement. MMs are a class of artificial matter composed of subwavelength unit cells, which may be termed meta-atoms. They are usually periodically arranged in space, hence forming a metacrystal. The appropriate meta-atom design permits us to control the interaction strength with the optical field and thus the optical response of the metamaterial. This response may exhibit a resonant behavior if elementary excitations such as plasmon polaritons are excited. Under certain conditions, the effective permittivity and permeability can be introduced, which exhibit near such resonances a strong dispersion and can become negative in the same spectral domain. The implementation of optical elements or devices based on such MMs requires one to understand light propagation in bulk MMs for any angle of incidence (or lateral wave vector component), including the transition conditions between different MMs and/or MMs and conventional dielectric materials.

A brute force approach toward modeling the light propagation in MMs is to rigorously solve the macroscopic Maxwell's equations with an inhomogeneous permittivity  $\epsilon(x, y, z, \omega)$  by using standard numerical techniques as the Fourier modal method (FMM),<sup>3</sup> spectral domain finite ele-

ment method,<sup>4</sup> and finite difference time domain method.<sup>5</sup> However, all approaches require huge CPU and memory resources. A solution to this issue is provided by classical macroscopic electrodynamics. There microscopic material properties and fields are averaged over length scales, which may be as small as some nanometers, to introduce phenomenological, macroscopic dielectric and magnetic functions as the permittivity and the permeability. Only this simplification paved the way for the success of electrodynamics and optics in effectively describing the field evolution in matter.

A similar procedure can be applied in MMs, provided that the wavelength is much larger than the period of the meta-atom's arrangement, and consists in averaging over an ensemble of meta-atoms yielding effective parameters and fields for a *homogeneous* MM. However, care has to be taken regarding several aspects. First, for periodically arranged meta-atoms, the field in the MM (in the quasimicroscopic picture) can be represented as an ensemble of Bloch modes, which are the normal modes of any periodic system. Due to the small period, only the zeroth order mode will be nonvanishing. However, under certain circumstances, and usually in bulk MMs, higher order modes can be excited with even larger amplitudes than the zeroth order one and will essentially contribute to the field evolution.<sup>6</sup> In this case, the averaging process fails to provide reasonable results and homogenization is not possible. Usually these modes can be suppressed by reducing the coupling between the meta-atoms.<sup>6</sup> If this is the case, the resulting effective parameters do not depend on the spatial coordinates and the normal modes in this medium are plane waves. Second, however, in general, the complex MM structure will not lead to global effective *material* parameters (refractive index, impedance, permittivity, and permeability). Because the retrieved parameters are directly related to a particular field, a plane wave, which propagates into a definite direction through the medium but only indirectly to the medium itself, they may be termed *wave* parameters.<sup>7,8</sup> These wave parameters will depend on the actual lateral wave vector. To date, to our best knowledge, there is no access to genuine material parameters of metamaterials. This would require *ab initio* calculations for an electron gas, confined in the meta-atom, in very large

systems (in terms of solid-state theory), which exceeds by far the current CPU performance. Up until now, the distinction between material and wave parameters did not play a significant role in the literature because only normal incidence of a plane wave, i.e., one fixed lateral wave vector ( $k_{\perp}=0$ ), was considered. From the physical point of view, the dependence of optical parameters on the wave vector may originate from anisotropy<sup>9–12</sup> or spatial dispersion.<sup>7,13–17</sup> Nowadays, it has been suggested that in the available optical metamaterials, both effects will play their role. Glancing at implemented MM structures (split ring with wires, cut wires, and fishnet), anisotropy seems to be evident and, moreover, because the meta-atom period is only about a one-third of the wavelength, nonlocal effects (spatial dispersion) are very likely to appear, but this cannot be proven by *ab initio* calculations.

The technique to derive effective parameters we use is based on the simulated or measured complex reflection ( $R$ ) and transmission ( $T$ ) coefficients of a finite MM slab.<sup>9,18–20</sup> In this approach, the slab is assumed to be made of a homogeneous medium with complex permittivity and permeability. By inverting the analytical expressions for  $R$  and  $T$ , one can solve for the refractive index and the impedance. Then, these data can be straightforwardly used to calculate both the permittivity and the permeability.

This approach holds the potential to be extended toward the relevant case of oblique incidence, which is the subject of the present work. It will turn out that for both a given frequency and the continuous lateral wave vector component parallel to the MM surface, the basic quantity that can be retrieved will be the normal wave vector component. This is exactly the same quantity, which is obtained by solving the dispersion relation for the Bloch modes in a, strictly speaking infinite, periodic structure.<sup>8</sup> Thus, provided that the retrieval procedure converges with increasing MM thickness, which is usually the case for stacks of more than five MM layers,<sup>6</sup> the quality of this homogenization can be easily double checked by comparing the retrieved wave vector with that obtained by the dispersion relation.<sup>8</sup>

To sum up, at this stage, an appropriate computational tool, in our case FMM, is used to calculate  $R$  and  $T$ . From the perspective of metamaterials, which are formed of meta-atoms, this can be understood as the solution of the microscopic problem since light–meta-atom interactions are rigorously analyzed by solving the macroscopic Maxwell’s equations in a medium that comprises nanostructured metallic elements. The subsequently introduced effective parameters can then be regarded as a macroscopic level of description.

To date, the determination of angularly resolved effective MM parameters has not been addressed. As already mentioned, we have to distinguish neatly between material and wave parameters. For a conventional anisotropic medium, the wave parameters can be rather simply derived from the material parameters and such a pronounced distinction is usually not necessary. For MMs, however, where all effective parameters explicitly depend on  $\vec{k}$ , the link between material and wave parameters is not trivial at all. Only if the dispersion relation of the fundamental Bloch mode provides a spherical isofrequency shape, a *global* effective refractive index, which is likewise a material parameter, can be intro-

duced. This holds similarly for isofrequency surfaces that compare to those of uniaxial or biaxial crystals. In this case, two or three global indices might be meaningfully derived as material parameters, e.g., the elements of the permittivity tensor of an anisotropic medium.

If a simple set of material parameters cannot be derived, one has to resort to the wave parameters. These wave parameters describe light propagation in a MM on a phenomenological level rather than analyzing it on a microscopic scale. The MM is assumed to be homogeneous but features some peculiarities evoked by the nanostructure. These wave parameters can be retrieved and they will be useful for predicting the functionality of MMs in applications where obliquely incident fields matter. In this context, wave parameters are the longitudinal wave vector and a generalized impedance only. However, if they are known, the introduction of a formally correct permittivity and permeability is feasible. In the following, these parameters are likewise understood as wave parameters. This subtle distinction is introduced contrary to their conventional use because they are directly derived from other wave parameters. They are inappropriate for a global material description, but they may be beneficially used to describe light propagation in MMs. The question may arise why one uses this approach if the dispersion relation of the fundamental Bloch mode provides also the relevant normal wave vector component. The reason is twofold. First, the present approach holds for any MM thickness and does not require a quasi-infinite medium. Second, only this approach provides effective permittivities and permeabilities, even if they vary with the wave vector. These quantities are indispensably required for formulating the transition condition between unlike MMs or MMs and conventional dielectric media.

It is the aim of this paper to put forward an approach for retrieving these angle- and polarization-dependent wave properties of MMs. The paper is structured as follows. In Sec. II, we shall derive equations for the normal component of the wave vector  $k_z$  and a generalized impedance. These quantities may then be used to derive the effective parameters  $\varepsilon$  and  $\mu$  which will depend on the angle of incidence and the polarization. In Sec. III, the procedure is applied to the fishnet MM. This geometry was chosen because at present it constitutes the most promising variant of a negative refractive index material with relatively low losses at optical frequencies. Issues that arise in assigning an effective refractive index, which is basically not required for describing light propagation in MMs, are revealed. Therefore, in Sec. IV, we shall finally discuss the relevance of the effective parameters introduced in this paper.

## II. RETRIEVAL PROCEDURE

In the present retrieval procedure, the MM is considered to be a homogeneous slab of thickness  $d$ . The pertinent geometry is shown in Fig. 1. The unit cells are periodically arranged in the  $x$  and  $y$  directions and the lattice axes coincide with the coordinate axes. The slab’s normal points into the  $z$  direction. The plane of incidence is the  $x$ - $z$  plane and the incidence angle is defined by the angle between the wave

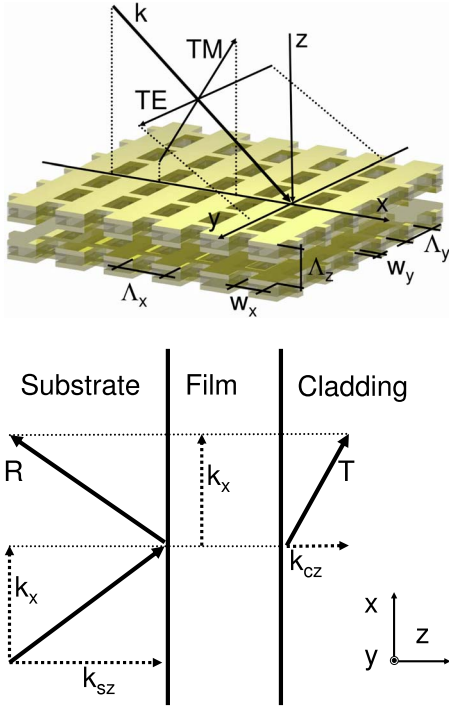


FIG. 1. (Color online) Sketch of the geometry under consideration. Top: the fishnet structure and the definition of the polarization. Bottom: cross section through the MM slab and definition of the wave vector components.

vector  $\vec{k}$  and the  $z$  axis. The electric (magnetic) field vector  $\vec{E}$  ( $\vec{H}$ ) is parallel to the  $y$  axis for TE (TM) polarization and remains in plane upon reflection and/or transmission. The restriction to these two principal polarizations is the only fundamental limitation we impose in our retrieval approach. Therefore, the effective parameters will be calculated only for the case  $k_y=0$ . Upon interaction with the structure, the linear polarization of the light field along one coordinate axis has to be preserved to ensure the required isotropy of the medium.

The transmission coefficient as derived from the standard  $2 \times 2$  transfer matrices<sup>21</sup> is given by

$$T = \frac{2\alpha^s k_z^s A}{(\alpha^s k_z^s + \alpha^c k_z^c) \cos(k_z^f d) - i \left( \alpha^f k_z^f + \frac{\alpha^s k_z^s \alpha^c k_z^c}{\alpha^f k_z^f} \right) \sin(k_z^f d)}, \quad (1)$$

where  $k_z^i(k_x, \omega) = \sqrt{\frac{\omega^2}{c^2} \epsilon^i(k_x, \omega) \mu^i(k_x, \omega) - k_x^2}$  is the normal component of the wave vector in medium ' $i$ ' and  $k_x$  is the tangential component of the wave vector. The superscripts  $i \in \{s, f, c\}$  denote substrate, film, and cladding, respectively. We note that  $k_z^i$ ,  $\epsilon^i$ , and  $\mu^i$  are scalar quantities that may explicitly depend on  $k_x$  and  $\omega$ , although for the substrate and the cladding, the  $k_x$  dependence can be usually dropped. For simplicity, in most cases, this dependence is not explicitly indicated; however, it is always kept in mind. The tangential component  $k_x$  is preserved in all spatial domains because of

the required homogeneity. The coefficients  $\alpha^i(k_x, \omega)$  depend on the polarization and are defined as

$$\text{TE: } \alpha^i(k_x, \omega) = \frac{1}{\mu^i(k_x, \omega)}, \quad \text{TM: } \alpha^i(k_x, \omega) = \frac{1}{\epsilon^i(k_x, \omega)}. \quad (2)$$

Since the transmission is defined by the ratio of the electric fields, the factor  $A$  in Eq. (1) amounts to  $A=1$  (TE polarization) or  $A = \sqrt{\epsilon^s \mu^c / \epsilon^c \mu^s}$  (TM polarization). The reflection coefficient  $R$  is given by

$$R = \frac{(\alpha^s k_z^s - \alpha^c k_z^c) \cos(k_z^f d) + i \left( \alpha^f k_z^f - \frac{\alpha^s k_z^s \alpha^c k_z^c}{\alpha^f k_z^f} \right) \sin(k_z^f d)}{(\alpha^s k_z^s + \alpha^c k_z^c) \cos(k_z^f d) - i \left( \alpha^f k_z^f + \frac{\alpha^s k_z^s \alpha^c k_z^c}{\alpha^f k_z^f} \right) \sin(k_z^f d)}. \quad (3)$$

By using the abbreviation  $k_{s,c} = \alpha^{s,c} k_z^{s,c}$  for the cladding and/or substrate quantities and by introducing the substitutions

$$k = k_z^f, \quad \xi = \alpha_f k_z^f,$$

we obtain expressions for  $T$  and  $R$  that can be analytically inverted,

$$T(k, \xi) = \frac{2k_s \xi A}{\xi(k_s + k_c) \cos(kd) - i(\xi^2 + k_s k_c) \sin(kd)}, \quad (4)$$

$$R(k, \xi) = \frac{\xi(k_s - k_c) \cos(kd) + i(\xi^2 - k_s k_c) \sin(kd)}{\xi(k_s + k_c) \cos(kd) - i(\xi^2 + k_s k_c) \sin(kd)}. \quad (5)$$

The slab is then fully characterized by the normal wave vector component  $k$  and the generalized impedance  $\xi$ . By inverting Eqs. (4) and (5), one obtains

$$kd = \pm \arccos \left( \frac{k_s(1 - R^2) + k_c(T/A)^2}{(T/A)[k_s(1 - R) + k_c(1 + R)]} \right) + 2m\pi, \quad (6)$$

with  $m \in \mathbb{Z}$  and

$$\xi = \pm \sqrt{\frac{k_s^2(R - 1)^2 - k_c^2(T/A)^2}{(R + 1)^2 - (T/A)^2}}. \quad (7)$$

For normal incidence and a slab embedded in vacuum, Eqs. (6) and (7) reduce to Eqs. (4)–(6) of Ref. 18. The signs of  $k$  and  $\xi$  can be chosen independently. They are unambiguously fixed on the base of physical considerations.

At first, to ensure an exponential decay for light propagating in the positive  $z$  direction, the imaginary part of  $k$  has to be always positive. This fixes the sign in Eq. (6). Furthermore, both the real and the imaginary parts of the normal component of the wave vector have to be continuous functions. Therefore, the order  $m$  is chosen as such to ensure this continuity. By starting the retrieval in the limit  $\lambda \rightarrow \infty$ , the branch  $m=0$  is selected. Subsequently reducing the wavelength and adjusting the branch number to obtain continuity for the normal component of the wave vector permits us to retrieve effective parameters for MM slabs of arbitrary (but

finite) thickness at arbitrary wavelengths. The choice of the sign of  $\xi$  appears more involved. In the case of normal incidence,  $\xi(k_x, \omega) = \alpha^f(k_x, \omega)k(k_x, \omega)$  is related to the impedance  $Z$  of the film by

$$\text{TE: } \xi(0, \omega) = \frac{1}{Z} \frac{\omega}{c}, \quad \text{TM: } \xi(0, \omega) = Z \frac{\omega}{c}. \quad (8)$$

For normal incidence, the sign of  $\xi$  is therefore unambiguously determined by the condition  $\text{Re}(Z) > 0$ . This is required for a passive medium. Throughout this work, the sign of  $Z$  is chosen such that its real part is positive. Therefore, starting our calculations from normal incidence allows us to determine the sign of Eq. (7) for  $k_x = 0$ . Depending on the polarization,  $\xi$  is related to the effective permittivity  $\mu$  (TE polarization) or to the effective permeability  $\varepsilon$  (TM polarization) by

$$\text{TE: } \xi(k_x, \omega) = \frac{k}{\mu(k_x, \omega)}, \quad \text{TM: } \xi(k_x, \omega) = \frac{k}{\varepsilon(k_x, \omega)}, \quad (9)$$

respectively. Since both effective parameters and the normal component of the wave vector have to be continuous, the sign of  $\xi$  has to be chosen by continuity arguments if one aims at calculating  $\xi(k_x, \omega)$ .<sup>22</sup>

Up to this point, the signs of the retrieved quantities  $k$  and  $\xi$  are chosen on physical grounds and both are continuous functions. To sum up,  $k$ ,  $\xi$ , and  $\mu$  [from Eq. (9)] for TE polarization and  $k$ ,  $\xi$ , and  $\varepsilon$  for TM polarization are now known. Finally, the missing effective parameters can be calculated by

$$\begin{aligned} \text{TE: } \frac{\omega^2}{c^2} \varepsilon(k_x, \omega) &= \frac{k_x^2 + k^2(k_x, \omega)}{\mu(k_x, \omega)}, \\ \text{TM: } \frac{\omega^2}{c^2} \mu(k_x, \omega) &= \frac{k_x^2 + k^2(k_x, \omega)}{\varepsilon(k_x, \omega)}. \end{aligned} \quad (10)$$

Formally, we can also introduce an effective refractive index  $n$  as

$$n(k_x, \omega) = \pm \frac{\sqrt{k^2(k_x, \omega) + k_x^2}}{\omega/c}. \quad (11)$$

For normal incidence, the sign of  $n$  has to be the same as the sign of  $k$  by writing  $k = n\omega/c$ . There are no further constraints for choosing the sign of the square root in Eq. (11).

There is no particular need to introduce this refractive index because all details of wave propagation follow from  $k(k_x, \omega)$ ,  $\varepsilon(k_x, \omega)$ , and  $\mu(k_x, \omega)$ . Particularly, for oblique incidence,  $n$  may lose its physical meaning and may even become discontinuous, as already shown in Ref. 8. This is due to the branch cut of the complex square root. Throughout this work, the sign of  $n$  is chosen such that the imaginary part of  $n$  is positive.

Note that all effective parameters are derived from the wave parameters  $k$  and  $\xi$ . Hence, they have to be likewise understood as wave parameters rather than as material parameters. In analogy to Eq. (11), we introduce the impedance as the last parameter of interest,

$$Z(k_x, \omega) = \pm \sqrt{\frac{\mu(k_x, \omega)}{\varepsilon(k_x, \omega)}}. \quad (12)$$

Here, the sign is chosen just as in Eq. (11), but  $\text{Re}(Z) > 0$  is always enforced.

### III. APPLICATION TO THE FISHNET STRUCTURE

To obtain negative refraction, various approaches for the MM design were proposed.<sup>23–28</sup> One of them is the fishnet structure. This structure attracts particular attention because it allows us to observe negative refraction in the visible, provides low losses, and can be potentially stacked to form a bulklike MM. That is why this structure is looked at in detail here. The basic geometry of the fishnet MM along with the definition of all relevant geometrical parameters, which correspond to the ones reported in the literature,<sup>29</sup> is shown in Fig. 1. The fishnet consists of three layers made of Ag-MgF<sub>2</sub>-Ag. The layers have thicknesses of  $h_{\text{Ag}} = 45$  nm and  $h_{\text{MgF}_2} = 30$  nm. The fishnet wires have widths of  $w_x = 100$  nm and  $w_y = 316$  nm. The periods were chosen to be  $\Lambda_x = \Lambda_y = 600$  nm and  $\Lambda_z = 200$  nm. For convenience, the stacked fishnets are separated by air. The Drude model, which provides an adequate description in the spectral range of interest,<sup>29</sup> was used for the dielectric function of Ag,

$$\varepsilon_{\text{Ag}} = 1 - \frac{\omega_p^2}{\omega(\omega + i\omega_c)}, \quad (13)$$

where the plasma and the collision frequency are  $\omega_p = 1.37 \times 10^{16}$  s<sup>-1</sup> and  $\omega_c = 8.5 \times 10^{13}$  s<sup>-1</sup>, respectively. The refractive index of MgF<sub>2</sub> was set to be 1.38. These specific structural parameters are of minor importance and affect only the resonance strength and position in the dispersion of the effective parameters, not the physical conclusions to be drawn.

To date, in most cases, single MM layer structures are considered. By assigning effective parameters to a multiple layer slab, the convergence of the retrieved parameters with an increasing number of layers has to be ensured.<sup>6,8,18</sup> Genuine effective parameters have to be independent of the number of layers that form the MM.<sup>6,30</sup> The stronger the damping of higher order Bloch modes and the less they are excited, the better the effective parameters of a single layer match the effective parameters of the multilayer slab. Figure 2 shows the effective permittivity  $\varepsilon$ , the effective permeability  $\mu$ , the effective normal component of the wave vector  $k$ , the effective refractive index  $n$ , and the effective impedance  $Z$  exemplarily for TE-polarized light and for a transverse wave vector of  $k_x = 0.8727 \mu\text{m}^{-1}$  (corresponding to an incidence angle of 13.36° at  $\bar{\nu} = 1/\lambda = 6000$  cm<sup>-1</sup>). Results are shown as a function of the wave number. Here, we shall only present results for TE-polarized light since the procedure is analogous for TM polarization, thus yielding no further insight. However, the retrieved parameters also depend on polarization since the structure is anisotropic.

The complex coefficients  $R$  and  $T$  were calculated with the Fourier modal method.<sup>3</sup> The effective parameters are shown as a function of the number of MM layers where up to

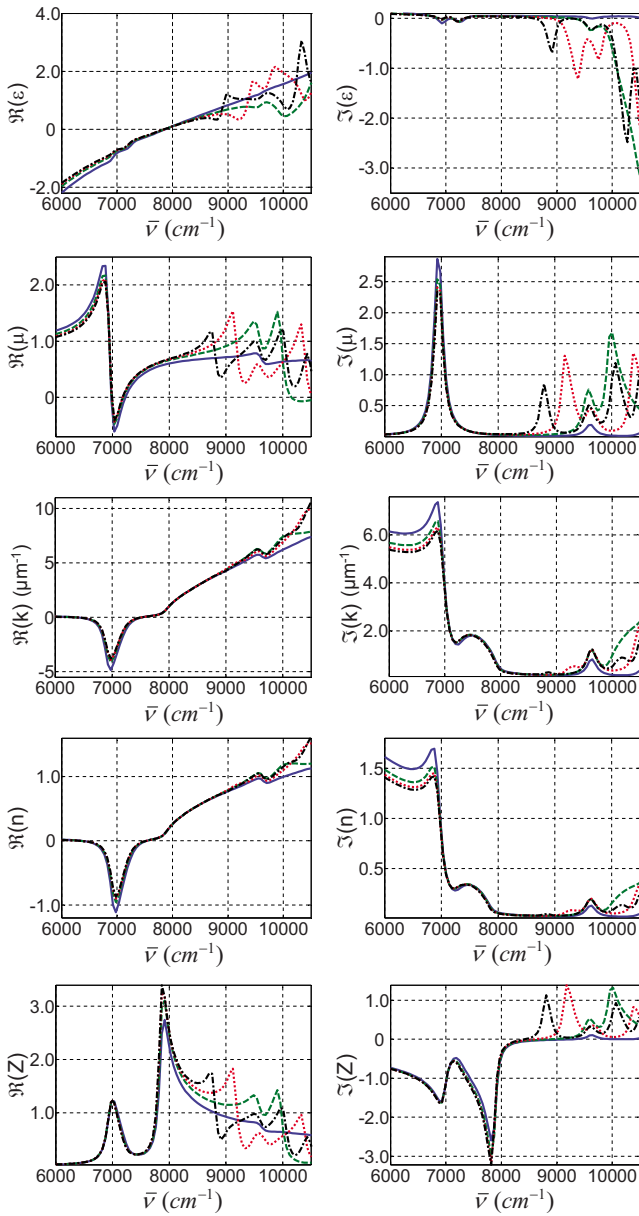


FIG. 2. (Color online) Real and imaginary parts of the effective permittivity  $\epsilon$ , the effective permeability  $\mu$ , the effective normal component  $k$  of the wave vector, the effective refractive index  $n$ , and the effective impedance  $Z$  as a function of the wave number and the number of MM layers. The results are shown at a fixed transverse wave number of the incident field of  $k_x=0.8727 \mu\text{m}^{-1}$  and TE polarization. The lines are labeled as follows: 1 MM layer—blue solid line, 2 MM layers—green dashed line, 3 MM layers—red dotted line, and 4 MM layers—black dashed-dotted line.

four layers were considered. The convergence of the effective parameters for an increasing number of layers is excellent for small wave numbers, i.e., large wavelengths, whereas effective bulk parameters for wave numbers larger than  $\bar{\nu}=8500 \text{ cm}^{-1}$  cannot be assigned because of the bad convergence.

While the convergence for larger wave numbers is acceptable for  $k$  and  $n$  too, the effective  $\epsilon$ ,  $\mu$ , and  $Z$  are strongly affected by reflections within the multilayer structure. The larger the number of layers, the more peaks were observed.

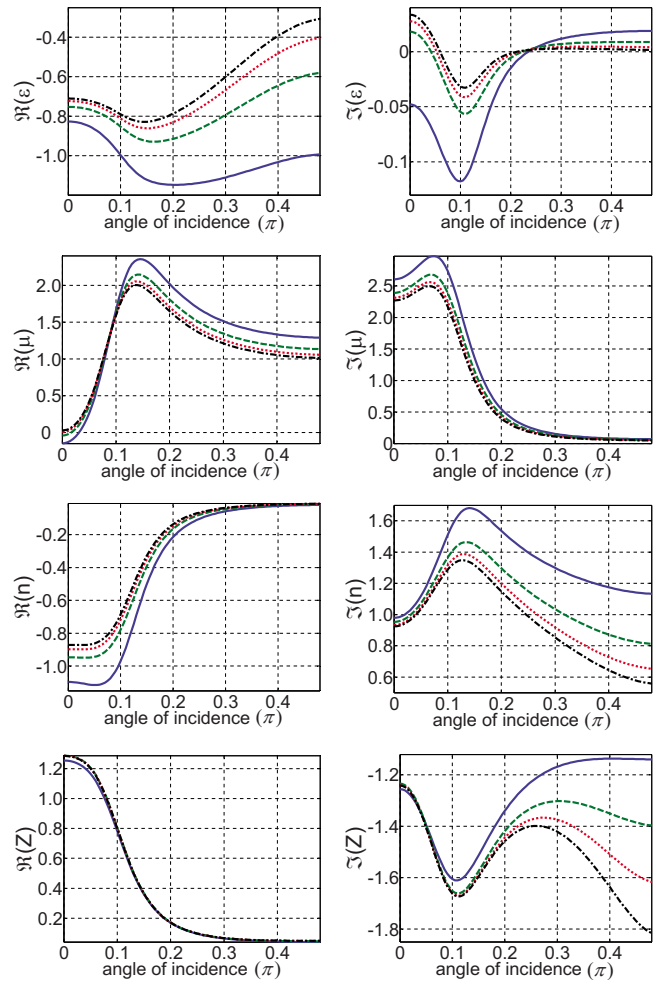


FIG. 3. (Color online) Real and imaginary parts of the effective permittivity  $\epsilon$ , the effective permeability  $\mu$ , the effective refractive index  $n$ , and the effective impedance  $Z$  as a function of the angle of incidence for different numbers of the MM layers. Results are shown for a fixed wave number of  $\bar{\nu}=6957 \text{ cm}^{-1}$ . The lines are labeled as follows: 1 MM layer—blue solid line, 2 MM layers—green dashed line, 3 MM layers—red dotted line, and 4 MM layers—black dashed-dotted line.

By contrast, the phase of the transmitted field governed by  $k$  is dominated by the field leaving the MM after a single passage. This is because of the strong absorption of the MM. Therefore, these waves are only slightly affected by multiple reflections and the convergence suffers only marginally.

Around  $\bar{\nu}=7000 \text{ cm}^{-1}$ ,  $k$  and, likewise,  $n$  become negative, where  $n$  reaches almost  $n=-1$ . This resonance can be primarily attributed to the strong Lorentzian dispersion in the effective permeability  $\mu$  induced by the coupled cut wires which form the fishnet. This yields a negative refractive index because the effective permittivity is likewise negative. The resonance at  $\bar{\nu}=7000 \text{ cm}^{-1}$  is accompanied by a strong imaginary part in both  $\mu$  and  $n$ . Since  $k_x$  is small in comparison to the wave number  $\bar{\nu}$ , light propagation is dominated by  $k$  and therefore the spectral dependence of  $n$  is quite similar to the spectral dependence of  $k$ . Note that the imaginary part of the permittivity  $\epsilon$  exhibits slightly negative values where  $\mu$  is resonant. These slightly negative values are usually

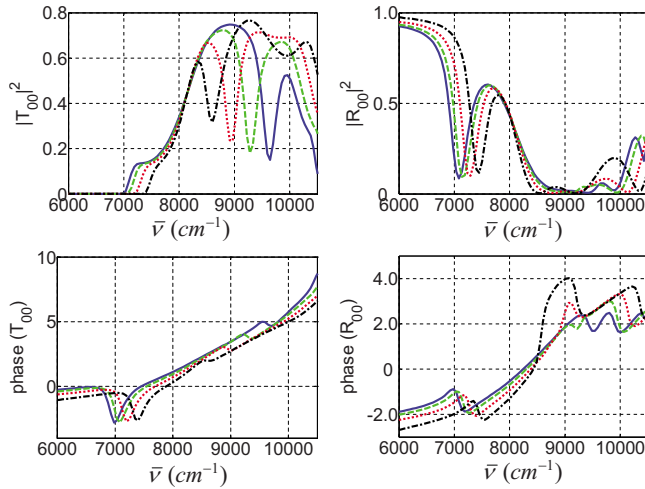


FIG. 4. (Color online) Amplitude and phase of the transmitted and reflected waves at a MM slab made of four layers as a function of the wave number for various transverse wave vector components  $k_x$ . The lines are labeled as follows:  $k_{x1}=0.8727 \mu\text{m}^{-1}$ —blue solid line,  $k_{x2}=2k_{x1}$ —green dashed line,  $k_{x3}=3k_{x1}$ —red dotted line, and  $k_{x4}=4k_{x1}$ —black dashed-dotted line.

called antiresonances. They are accompanied by an anti-Lorentzian shaped real part.

Furthermore, we investigated the dependence of the retrieved parameters on the angle of incidence in more detail. The results are shown in Fig. 3. The wavelength was fixed to  $\lambda=1.4373 \mu\text{m}$ , which corresponds to a wave number of  $\bar{\nu}=6957 \text{ cm}^{-1}$  where the refractive index attains its minimum ( $n \approx -1$ ) for normal incidence.

Again, the results are shown as a function of the number of MM layers to evaluate the convergence. Good convergence is generally observed. We conclude that four MM layers are sufficient to introduce bulk parameters, although the convergence is worse for larger angles of incidence.

All effective parameters  $\epsilon$ ,  $\mu$ ,  $n$ , or  $Z$  strongly depend on the incidence angle. Particularly, the real part of the effective refractive index  $n$  tends rapidly toward zero. A strong imaginary part is left due to the negative real part of  $\epsilon$ . For larger angles of incidence, the system behaves like a metal. It is interesting to note that the normal component of the wave vector is not altered that much by the change in  $k_x$  as one would expect for an isotropic medium. Therefore, the retrieved effective parameters become strongly angle dependent, as can be seen from Eq. (11).

Next, we investigated the dependence of the effective parameters on the wave number  $\bar{\nu}$  for some discrete values of  $k_x$  and a fixed number of layers. The amplitude of the transmitted and reflected waves and their respective phases are shown in Fig. 4. The effective parameters that can be retrieved from these complex amplitudes are shown in Fig. 5. By using four layers of the MM, we assume that it is guaranteed that the parameters converged sufficiently toward the bulk values of the MM. As already mentioned, the phase of the transmitted field is dominated by the single path contribution. Therefore, by investigating the phase of the transmitted field, the effective normal component of the wave vector is almost determined. Clearly, the interesting resonance that

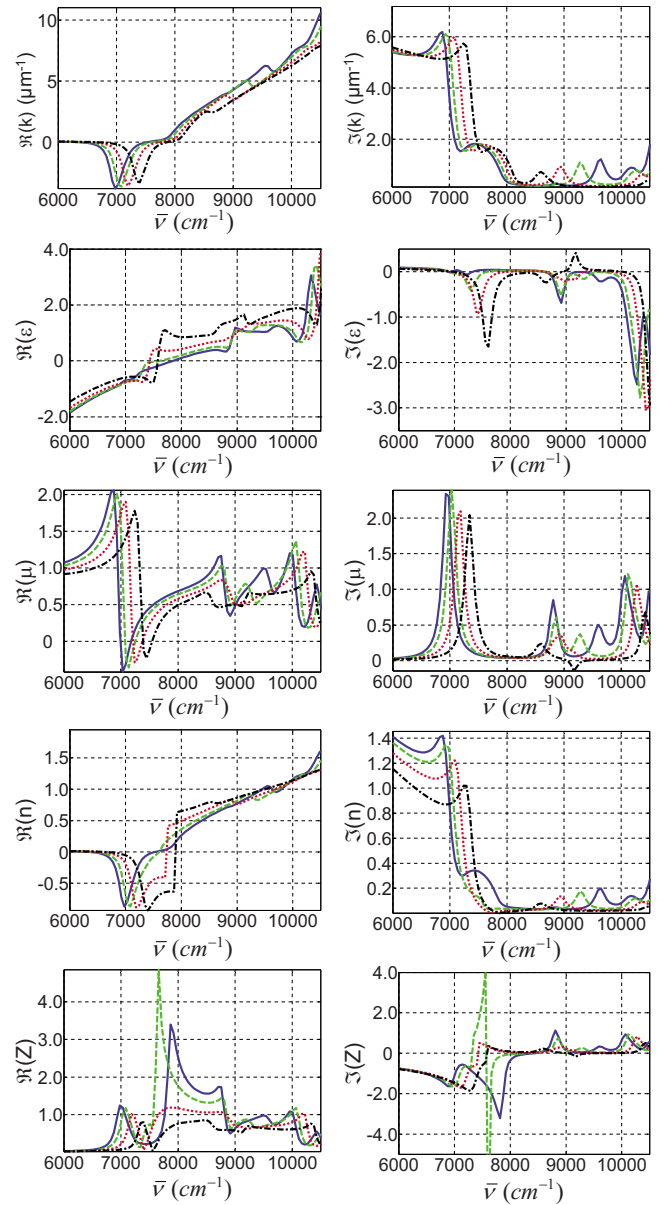


FIG. 5. (Color online) Real and imaginary parts of the permittivity  $\epsilon$ , the permeability  $\mu$ , the effective normal component  $k$  of the wave vector, the refractive index  $n$ , and the impedance  $Z$  versus the wave number  $\bar{\nu}=1/\lambda$  for different values of  $k_x$ . The lines are labeled as follows:  $k_{x1}=0.8727 \mu\text{m}^{-1}$ —blue solid line,  $k_{x2}=2k_{x1}$ —green dashed line,  $k_{x3}=3k_{x1}$ —red dotted line,  $k_{x4}=4k_{x1}$ —black dashed-dotted line.

causes the effective index to be negative is shifted toward higher wave numbers with an increasing transverse wave vector component. The resonances corresponding to multiple reflections, which appear at larger wave numbers, are shifted toward smaller wave numbers with increasing  $k_x$ . We furthermore observe that the antiresonance in the permittivity  $\epsilon$  is more pronounced for larger values of  $k_x$  while the resonance in  $\mu$  is slightly decreased. Note that the parameters  $\epsilon$  and  $\mu$  are continuous and behave as expected. On the contrary, the effective refractive index exhibits a quite strange behavior for increasing  $k_x$ , i.e., at a certain value of  $k_x$ , continuity requires us to select the lower branch of Eq. (11). Since there

is no physical constraint for the sign of  $n$ , both solutions are equal and indistinguishable. Although this sounds counterintuitive, there is no physical problem at all. As mentioned above, the refractive index has no physical meaning for oblique incidence. Only the square of  $n$  as the product of  $\epsilon$  and  $\mu$  enters the equations describing the propagation of light. The sign of  $n$  is of importance only if a meaningful refractive index at normal incidence should be introduced. We decided to extend the need for the imaginary part of  $n$  to be positive. This results in a discontinuity of  $\text{Re}(n)$  and a kink of  $\text{Im}(n)$ . The problem behind this behavior was described when  $n$  was introduced [see Eq. (11)].

So the question arises if the introduction of  $n$  is useful at all. The refractive index is usually introduced if the product of  $\epsilon$  and  $\mu$  is independent of the wave vector  $\vec{k}$ . Even for birefringent media, the index is only slightly varying with  $\vec{k}$ , i.e., the refractive index manifold is given by an ellipsoid. If  $n$  is rapidly varying with the lateral wave vector component  $k_x$ , its introduction is questionable since there is no simplification for understanding the light propagation in such media. This problem will be encountered in describing light propagation in almost all MMs proposed so far.

The results presented in this work clearly show that all retrieved parameters strongly depend on  $k_x$ . As discussed earlier, this dependence is caused by anisotropy and spatial dispersion. The effective parameters do not represent the physical material but only the wave parameters. These wave parameters provide the complex transmission and reflection coefficients at a MM slab by assuming that the real MM is conceptually replaced by a homogeneous medium. Thus, their use significantly simplifies the description of the prob-

lem as one does not need to compute the involved light interaction with a nanostructured medium. Instead, one may resort to simple transfer matrix techniques for stratified media. This simplification is the very reason for the introduction of effective wave parameters.

#### IV. CONCLUSION

In conclusion, this work represents a further step toward the design and the optical characterization of MMs to be tailored for unprecedented applications. To this end, an extension of the well-known parameter retrieval procedure toward oblique incidence has been introduced. This provides the opportunity to straightforwardly characterize the optical properties of MMs by effective parameters. The physical meaning of the retrieved parameters was discussed in detail. It has been emphasized that only the normal components of the wave vector  $k$ , the permeability  $\mu$ , and the permittivity  $\epsilon$  are physically meaningful quantities. The introduction of an effective refractive index provides no further insight into the issue but may, e.g., serve to double check the MM for engineered isotropy. The general results have been applied to the fishnet structure, which is highly relevant for applications.

#### ACKNOWLEDGMENTS

Parts of the computations were performed on the IBM p690 cluster (JUMP) of the Forschungs-Zentrum in Jülich, Germany. The authors acknowledge support by the Federal Ministry of Education and Research (Unternehmen Region, ZIK ultra optics).

\*christoph.menzel@uni-jena.de

<sup>1</sup>J. B. Pendry, Phys. Rev. Lett. **85**, 3966 (2000).

<sup>2</sup>N. Engheta and R. Ziolkowski, *Metamaterials: Physics and Engineering Explorations* (IEEE, New York, 2006).

<sup>3</sup>L. Li, J. Opt. Soc. Am. A **14**, 2758 (1997).

<sup>4</sup>P. P. Silvester and R. L. Ferrari, *Finite Elements for Electrical Engineers*, 2nd ed. (Cambridge University Press, Cambridge, 1990).

<sup>5</sup>A. Taflov and S. C. Hagness, *Computational Electrodynamics: The Finite-Difference Time-Domain Method* (Artech House, Boston, 2000).

<sup>6</sup>C. Rockstuhl, T. Paul, F. Lederer, T. Pertsch, T. Zentgraf, T. P. Meyrath, and H. Giessen, Phys. Rev. B **77**, 035126 (2008).

<sup>7</sup>A. I. Cabuz, D. Felbacq, and D. Cassagne, Phys. Rev. A **77**, 013807 (2008).

<sup>8</sup>C. Rockstuhl, C. Menzel, T. Paul, T. Pertsch, and F. Lederer, (unpublished).

<sup>9</sup>X. Chen, B.-I. Wu, J. A. Kong, and T. M. Grzegorzczak, Phys. Rev. E **71**, 046610 (2005).

<sup>10</sup>Qiang Cheng and Tie Jun Cui, Phys. Rev. B **73**, 113104 (2006).

<sup>11</sup>P. A. Belov, C. R. Simovski, and S. A. Tretyakov, Phys. Rev. E **67**, 056622 (2003).

<sup>12</sup>I. V. Lindell, A. H. Shivola, S. A. Tretyakov, and A. J. Viitanen, *Electromagnetic Waves in Chiral and Bi-Isotropic Media*

(Artech House, Boston, 1994).

<sup>13</sup>M. G. Silveirinha, Phys. Rev. B **75**, 115104 (2007).

<sup>14</sup>M. A. Shapiro, G. Shvets, J. R. Sirigiri, and R. J. Temkin, Opt. Lett. **31**, 2051 (2006).

<sup>15</sup>P. A. Belov, R. Marqués, S. I. Maslovski, I. S. Nefedov, M. Silveirinha, C. R. Simovski, and S. A. Tretyakov, Phys. Rev. B **67**, 113103 (2003).

<sup>16</sup>R. Marqués, F. Medina, and R. Rafii-El-Idrissi, Phys. Rev. B **65**, 144440 (2002).

<sup>17</sup>S. A. Tretyakov, *Analytical Modeling in Applied Electromagnetics* (Artech House, Boston, 2003).

<sup>18</sup>D. R. Smith, S. Schultz, P. Markoš, and C. M. Soukoulis, Phys. Rev. B **65**, 195104 (2002).

<sup>19</sup>D. R. Smith, D. C. Vier, T. Koschny, and C. M. Soukoulis, Phys. Rev. E **71**, 036617 (2005).

<sup>20</sup>X. Chen, T. M. Grzegorzczak, B.-I. Wu, J. Pacheco, and J. A. Kong, Phys. Rev. E **70**, 016608 (2004).

<sup>21</sup>P. Yeh, *Optical Waves in Layered Media* (Wiley, New York, 2005).

<sup>22</sup>K. Busch, G. v. Freymann, S. Linden, S. F. Mingaleev, L. Tkeshelashvili, and M. Wegener, Phys. Rep. **444**, 101 (2007).

<sup>23</sup>J. B. Pendry, A. J. Holden, D. J. Robbins, and W. J. Stewart, J. Phys.: Condens. Matter **10**, 4785 (1998).

<sup>24</sup>V. M. Shalaev, W. Chai, U. K. Chettiar, H.-K. Yuan, A. K. Sary-

- chev, V. P. Drachev, and A. V. Kildishev, *Opt. Lett.* **30**, 3356 (2005).
- <sup>25</sup>G. Dolling, C. Enkrich, M. Wegener, J. F. Zhou, C. M. Soukoulis, and S. Linden, *Opt. Lett.* **30**, 3198 (2005).
- <sup>26</sup>S. Zhang, W. Fan, K. J. Malloy, S. R. Brueck, N. C. Panoiu, and R. M. Osgood, *Opt. Express* **13**, 4922 (2005).
- <sup>27</sup>F. Garwe, C. Rockstuhl, C. Etrich, U. Hübner, U. Bauernschäfer, F. Setzpfandt, M. Augustin, T. Pertsch, A. Tünnermann, and F. Lederer, *Appl. Phys. B* **84**, 139 (2006).
- <sup>28</sup>M. Kafesaki, I. Tsiapa, N. Katsarakis, T. Koschny, C. M. Soukoulis, and E. N. Economou, *Phys. Rev. B* **75**, 235114 (2007).
- <sup>29</sup>G. Dolling, C. Enkrich, M. Wegener, C. M. Soukoulis, and S. Linden, *Opt. Lett.* **31**, 1800 (2006).
- <sup>30</sup>C. R. Simovski, S. A. Tretyakov, A. H. Sihvola, and M. Popov, *Eur. Phys. J.: Appl. Phys.* **9**, 195 (2000).